

Article

Phenylalanine-Rich Peptide Mediated Binding with Graphene Oxide and Bioinspired Synthesis of Silver Nanoparticles for Electrochemical Sensing

Li Wang * and Jing Lin

College of Chemistry, Jilin Normal University, Siping 136000, China; linjing@ciac.ac.cn

* Correspondence: liwang_jlnu@163.com; Tel.: +86-434-3292-154

Academic Editor: Gang Wei

Received: 3 January 2017; Accepted: 3 February 2017; Published: 8 February 2017

Abstract: We demonstrated that a phenylalanine-rich peptide molecule, (FEFEFKFK)₂, could be used for the biofunctionalization of graphene oxide (GO) and the bioinspired synthesis of silver nanoparticles (AgNPs) for the creation of functional GO–AgNPs nanohybrids. The successful synthesis of GO–AgNPs nanohybrids was proven by the characterizations of atomic force microscopy, transmission electron microscope, and X-ray photoelectron spectroscopy. The fabricated electrochemical H₂O₂ sensor based on the synthesized GO–AgNPs nanohybrids showed high performances with a linear detection range 0.02–18 mM and a detection limit of 0.13 μM. The design of graphene-binding peptides is of benefit to the biofunctionalization of graphene-based materials, the synthesis of novel graphene–peptide nanohybrids, and the potential applications of graphene in biomedical fields.

Keywords: graphene; peptide; bioinspired synthesis; silver nanoparticles; electrochemical sensor

1. Introduction

Carbon and metallic nanomaterials have shown wide applications in various fields from electrocatalysis [1,2], energy materials [3] and biosensors [4], to biomedical materials [5]. Graphene is a two-dimensional (2D) carbon material with monolayered hexagonal sp² hybridized carbons. It has attracted increasing attentions due to its uniform 2D structure, high conductivity, unique mechanical property, and large surface area [6–8]. To extend its potential applications in materials science, nanotechnology and biomedicine, many nanoscale building blocks such as nanoparticles (NPs) [2,9–11], quantum dots [12,13], biomolecules [4,14], polymers [15,16], and others have been utilized to conjugate with graphene to form graphene-based hybrid nanomaterials, which showed enhanced performances in comparison with sole graphene materials.

Both covalent and noncovalent methods could be used for the functionalization of graphene for further synthesis of graphene-based hybrid nanomaterials [17–20]. As the irreversible nature of these covalent bonds formed in the covalent modification process would potentially hinder the electronic properties of graphene, the noncovalent modifications, by using both π–π and electrostatic interactions, offer promising ways to achieve the plane-specific functionalization of the graphene surface [21–23]. Previously, a few sequence-designed peptides such as EPLQLKM, YWYAF, and GAMHLPWHMGTL with highly specific graphene-binding ability have been discovered through both experimental and theoretical studies [24–27]. In addition, the formed graphene–peptide nanohybrids have shown high potentials to fabricate graphene–NPs [23,28] and graphene–hydroxyapatite [22,29] nanohybrids for various biomedical applications.

In this work, we demonstrated that a phenylalanine (F)-rich peptide molecule with the amino acid sequence of (FEFEFKFK)₂ shows high binding affinity with graphene oxide (GO) nanosheets

by the noncovalent π - π interaction, which promotes the formation of a dense network-like peptide structure on both sides of GO nanosheets. The conjugated peptide molecules not only provide the nucleation and growth templates for the bioinspired synthesis of silver nanoparticles (AgNPs), but also serve as the bridges for connecting GO with the formed AgNPs to create GO-peptide-AgNPs nanohybrids. The synthesized GO-peptide-AgNPs nanohybrids were directly used to modify a glass carbon electrode (GCE) to fabricate a nonenzymatic electrochemical hydrogen peroxide (H_2O_2) sensor, which reveals high sensing performance with a detection limit of $0.13 \mu\text{M}$ and a wide linear range from 0.02 to 18 mM.

2. Materials and Methods

GO synthesized by the Hummers method was dissolved and dispersed in ultrapure water to a final concentration of 0.1 mg/mL. Peptide (>90% purity, JPT Company, Berlin, Germany) was dissolved in ultrapure water to a final concentration of 0.2 mg/mL. The typical process of peptide-mediated synthesis of GO-peptide-AgNPs nanohybrids is shown in Figure 1. Firstly, 5 mL GO and 1 mL peptide solutions were mixed under stirring, and then 4 mL ultrapure water was added into the mixed solution to keep the final volume at 10 mL. Secondly, after two hours, the mixed solution was centrifuged at a speed of 13 K to remove the unbound peptide, and the product was dissolved with ultrapure water to 5 mL. Then, 0.1 mL AgNO_3 with a concentration of 0.1 M was added to the GO-peptide solution under stirring and the pH of the mixed solution was adjusted to 2.0. Thirdly, after another two hours, the mixed solution was centrifuged again to remove the excessive Ag^+ and ultrapure water was added to keep the volume at 5 mL. Then, freshly prepared NaBH_4 (1%, *m/m*) was added drop by drop into the mixed solution to synthesize GO-peptide-AgNPs nanohybrids. After 10 min, the product was centrifuged and dissolved with water to a final volume of 2 mL for further characterizations and electrochemical tests.

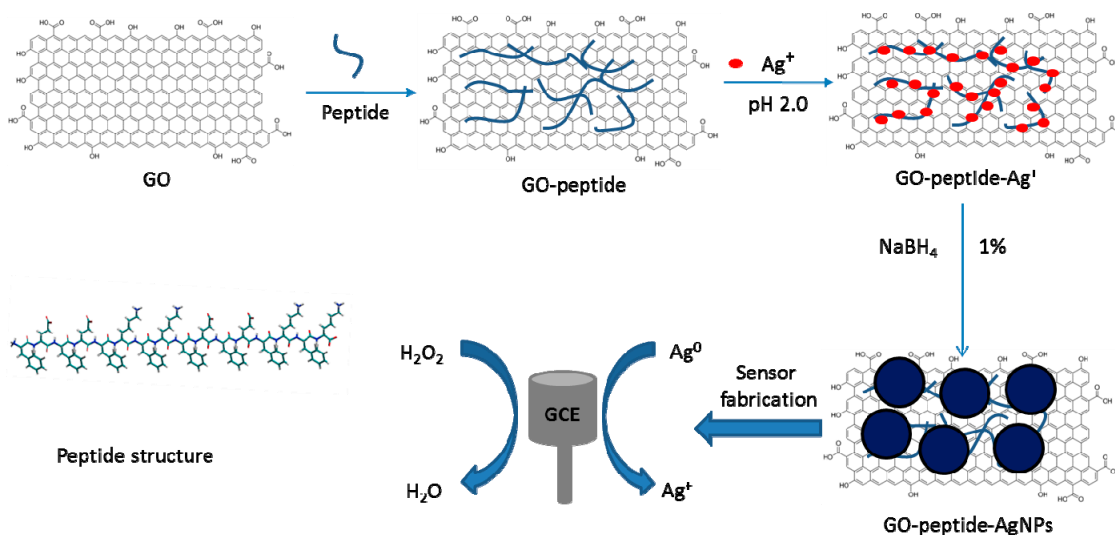


Figure 1. Schematic presentation on the peptide-mediated biomimetic synthesis of GO-peptide-AgNPs nanohybrids.

For the preparation of GO-peptide-AgNPs nanohybrids modified GCE, 0.1 mL GO-peptide-AgNPs nanohybrids solution was directly transferred onto the GCE surface and dried for cyclic voltammograms (CV) and amperometric response tests. All the electrochemical tests were carried out on an electrochemical workstation (CHI760D, Chenhua Company, Shanghai, China) with the conventional three-electrode system.

Atomic force microscopy (AFM) was conducted with a NanoWizard 3 NanoScience atomic force microscope (JPK Instruments AG, Berlin, Germany) at tapping mode. Transmission electron microscope

(TEM) characterization was carried out with a Tecnai G220 transmission electron microscope (FEI, Beijing, China) with an accelerating voltage of 200 kV. The chemical state of GO–AgNPs nanohybrids was measured by X-ray photoelectron spectroscopy (XPS, ThermoVG ESCALAB 250, Waltham, MA, USA).

3. Results

AFM was utilized to identify the successful binding of F-rich peptide onto the GO surface firstly. Figure 2a shows the typical AFM height image of peptides by dropping 10 μL peptide solution (20 $\mu\text{g}/\text{mL}$) onto the freshly cleaved mica surface. The adsorbed peptide molecules on the mica surface reveal dispersed sphere-like structure and the corresponding section analysis indicates that the height of peptide molecules is about 1.8 ± 0.2 nm. Figure 2b gives an AFM height image of GO nanosheets that deposited onto the mica surface, and the section analysis reveals that GO is in a monolayer with a uniform height of 1.2 ± 0.1 nm, which is in accordance with the previous report on the shape and size of GO nanosheets [30]. After binding peptides onto the GO surface, the mixed GO–peptide solution was still highly dispersed. The mono-dispersed GO–peptide nanohybrids were further observed with AFM (Figure 2c), and the section analysis shows that the formed GO–peptide has a mean height of 4.6 ± 0.3 nm, which is equal to the sum height value of monolayer GO (1.2 ± 0.1 nm) and two peptide molecules (1.8 ± 0.2 nm). Therefore, we suggest that the F-rich peptide molecules were bound onto both sides of GO due to the excessive amount of peptide and the high binding ability of F-rich peptide with GO. In addition, we found that a network-like peptide structure was formed on the GO surface (inset of Figure 2c), which means that the binding of peptide onto the GO surface changed the conformation of peptide and promoted their inter-molecular interactions.

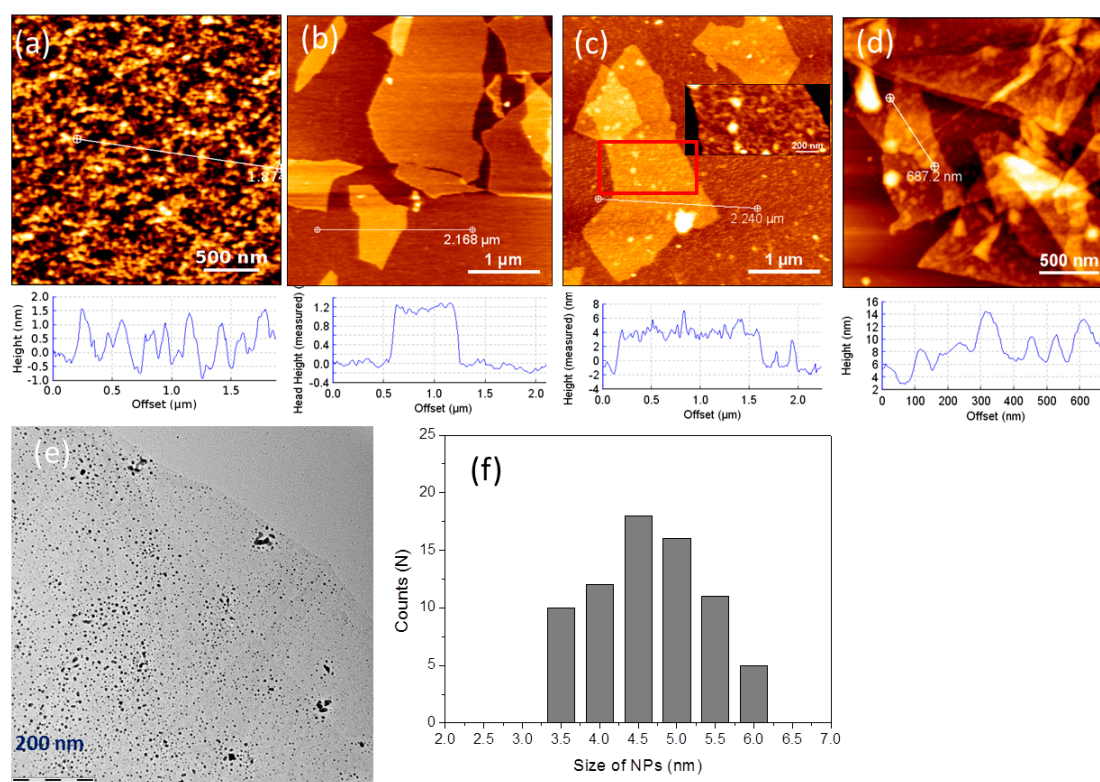


Figure 2. Morphological characterizations of materials: (a–d) AFM characterization of (a) peptide; (b) GO; (c) GO–peptide, the inset is the zoomed area of the red box; and (d) GO–peptide–AgNPs; (e) TEM image of AgNPs formed on the GO surface; (f) corresponding statistical analysis of the size of nanoparticles in (e).

Besides the biofunctionalization of GO, the bound peptides could also serve as nucleation and growth sites for the bioinspired synthesis of metallic nanoparticles [23]. Figure 2d shows the typical AFM height image of the created GO-peptide-AgNPs nanohybrids. It can be found that a lot of AgNPs were formed on the surface of GO nanosheets. The corresponding section and statistical analysis indicate that the synthesized AgNPs have a mean size of 5.4 ± 1.1 nm. TEM measurement was further utilized to observe the size of AgNPs that formed on the GO surface (Figure 2e), and the statistical analysis shows that the formed AgNPs have a mean size of 4.8 ± 1.4 nm (Figure 2f), which is in good agreement with the above AFM data.

It is very important to know the amount of peptide and AgNP loading on the GO surface in order to understand the interactions between the peptide and GO. We suggest that ultraviolet-visible spectrophotometry (UV-vis) may be a potential technique to measure the peptide loading on the GO surface by centrifuging the samples after peptide binding. In addition, it is also possible to know the loading of AgNPs onto the GO surface by simply measuring the mass of samples before and after adding Ag^+ and subsequent chemical reduction. All the data could be of benefit for the understanding of the adsorption kinetics of peptide onto the graphene surface.

XPS measurement was further utilized to prove the formation of GO-peptide-AgNPs nanohybrids. Figure 3 shows the XPS peaks of C1s, Ag3d, and N1s of the peptide-bioinspired GO-peptide-AgNPs nanohybrids. The strong C1s peak at 283.7 eV comes from the C contents of both GO and peptide molecules, and the appearance of the N1s peak at 398.8 eV is ascribed to the amino acid residue of peptide molecules [30]. In addition, two sharp peaks at 367.0 and 372.9 eV were found, which are assigned to the $\text{Ag}3d_{5/2}$ and $\text{Ag}3d_{3/2}$ peaks of AgNPs, respectively [31].

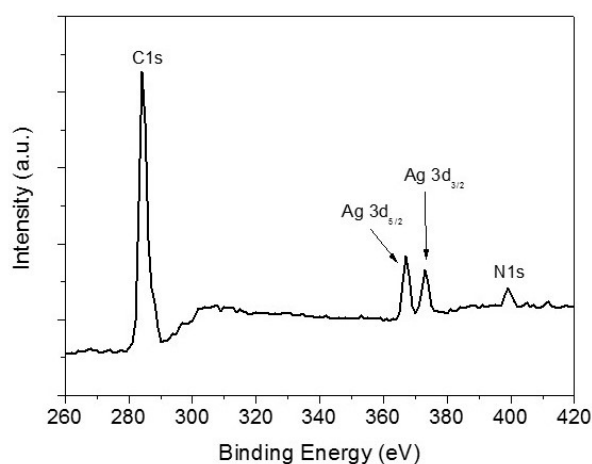


Figure 3. XPS spectrum of the C1s, Ag3d, and N1s peaks of GO-peptide-AgNPs nanohybrids.

In the current study, the potential application of GO-peptide-AgNPs nanohybrids for the fabrication of electrochemical H_2O_2 sensor was explored. To obtain an optimal applied potential for the sensor test, we measured the CVs of the fabricated GO-peptide-AgNPs/GCE by adding H_2O_2 with different concentrations (Figure 4). It can be found that a strong reduction peak at about -0.51 V appeared, which was then selected as the applied potential for the next current-time (I-T) measurement.

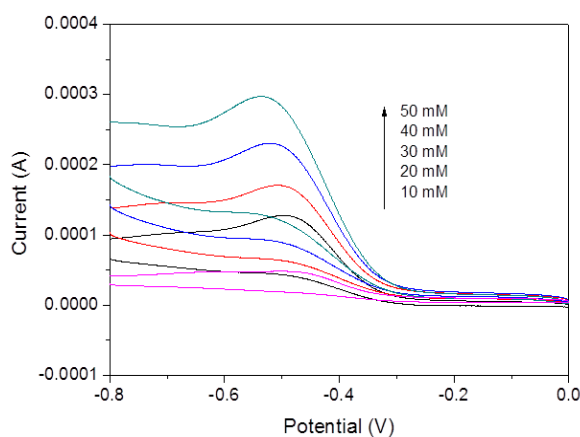


Figure 4. CVs of the fabricated GO-peptide-AgNPs/GCE by adding H₂O₂ with different concentrations.

Figure 5a displays a typical I-T curve with GO-peptide-AgNPs/GCE on successive additions of H₂O₂. It is clear that the addition of 20 μM H₂O₂ into the system caused a rapid current response. The corresponding calibration of the obtained I-T data indicates a regular response towards H₂O₂ with a linear detection range from 0.02 to 18 mM (Figure 5b). According to the linear fit, a detection limit of 0.13 μM with a sensitivity of 3.6 μA·mM⁻¹ was calculated (S/N = 3). To make it more clear, we compared the sensing performance of our H₂O₂ sensor based on GO-peptide-AgNPs nanohybrids with several reported sensors based on graphene-NPs [23,32–36], as shown in Table 1.

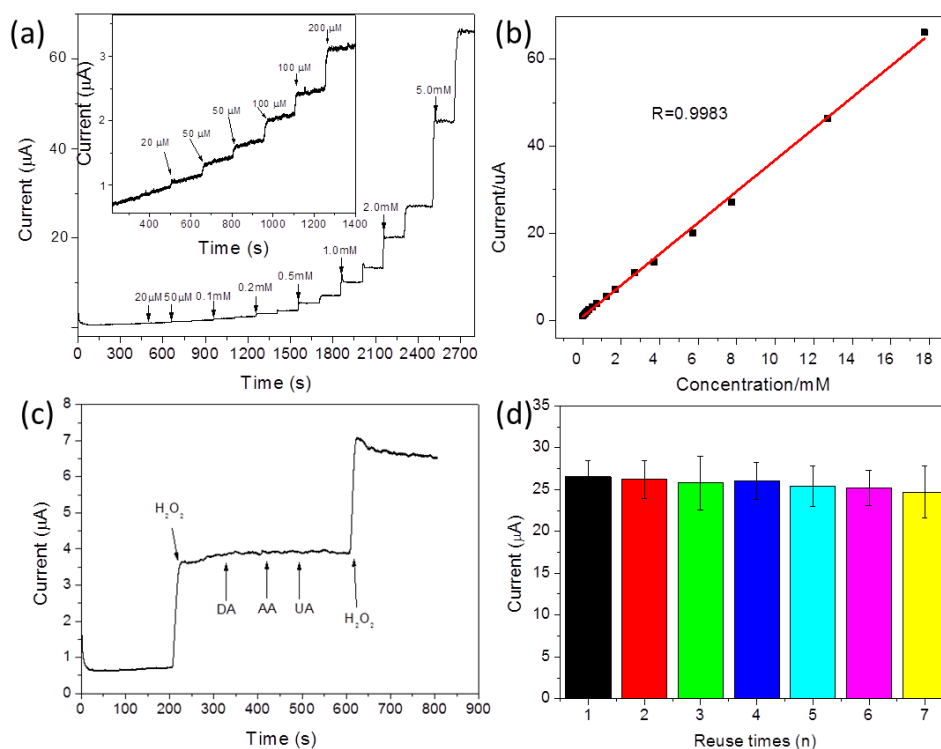


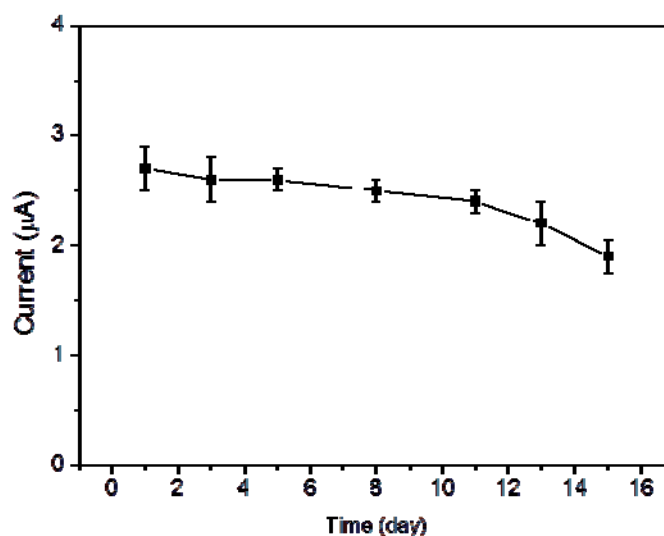
Figure 5. Performance of the H₂O₂ sensor based on GO-peptide-AgNPs nanohybrids: (a) I-T response; (b) calibration curve; (c) anti-interference capability; and (d) reuse stability.

Table 1. Comparison of electrochemical H₂O₂ sensors based on graphene-NPs nanohybrids.

Materials	Linear Range	Detection Limit	Reference
RGO-peptide nanofiber-AgNPs	0.05–5 mM	10.4 μM	[23]
RGO-Polymer-AgNPs	0.1–40 mM	28 μM	[32]
RGO-AuNPs	0.5 μM–0.5 mM	0.22 μM	[33]
RGO-AgNPs	0.1–100 mM	31.3 μM	[34]
Graphene/Au/horseradish peroxidase/chitosan	0.005–5.13 mM	1.7 μM	[35]
Hb/AuNPs/ZnO/RGO	0.006–1.13 mM	0.8 μM	[36]
GO-peptide-AgNPs	0.02–18 mM	0.13 μM	This work

Figure 5c shows the anti-interference test of the fabricated electrochemical sensor by adding three relevant electroactive species, dopamine (DA), ascorbic acid (AA), and uric acid (UA). It can be found that the addition of all species did not cause any current response, which identifies the high selectivity of the fabricated sensor based on GO-peptide-AgNPs nanohybrids towards the detection of H₂O₂. In addition, the reuse stability of the fabricated H₂O₂ sensor was investigated (Figure 5d). After using for seven times, the current response towards the same H₂O₂ concentration still kept more than 95% of the original value.

The further long-term stability test indicates that the fabricated H₂O₂ sensor based on GO-peptide-AgNPs nanohybrids can be stable stored at 4 °C for at least 13 days (Figure 6). Based on the above results, it can be concluded that this H₂O₂ sensor based on GO-peptide-AgNPs nanohybrids reveals high performances with low detection limit, strong selectivity, good reuse capability, and long-term stability.

**Figure 6.** Long-term stability of the biosensor based on GO-peptide-AgNPs nanohybrids.

We suggest that there are a few advantages to using this kind of sequence-designed peptide for biofunctionalization of GO or reduced GO (RGO) and subsequent bioinspired synthesis of NPs. Firstly, the design of peptide molecules with specific amino acids is helpful for the facile biofunctionalization of GO and RGO. Secondly, the introduction of peptide onto the GO or RGO surface can greatly improve the solubility and biocompatibility of graphene, and extend their biomedical and nanotechnological applications. Thirdly, the bound peptide molecules could serve as nucleation and growth templates for the formation of metallic or metallic oxide nanoparticles for electrochemical sensors and catalysis.

4. Conclusions

In summary, we demonstrated a facile green strategy to functionalize GO and synthesize GO-peptide-AgNPs nanohybrids by using an F-rich peptide. It can be found that this F-rich peptide not only shows high binding affinity with GO, but also serves as the nucleation and growth template for bioinspired synthesis of AgNPs. The fabricated electrochemical H₂O₂ sensor with the peptide-inspired GO-peptide-AgNPs nanohybrids exhibited high performance with a detection limit of 0.13 μM. It is expected that the strategies shown in this work such as the design of peptide structure, the biofunctionalization of GO, and the bioinspired synthesis of nanomaterials will be of benefit to the synthesis and applications of graphene-based hybrid nanomaterials in biomedical fields.

Acknowledgments: We acknowledge the financial support from the National Natural Science Foundation of China (Grant No. 21505049).

Author Contributions: Li Wang conceived and designed the experiments; Jing Lin performed the experiments; Li Wang and Jing Lin analyzed the data; Li Wang wrote the paper.

Conflicts of Interest: The authors declare no conflict of interest.

References

1. Sun, M.; Dong, Y.Z.; Zhang, G.; Qu, J.H.; Li, J.H. Alpha-Fe₂O₃ spherical nanocrystals supported on CNTs as efficient non-noble electrocatalysts for the oxygen reduction reaction. *J. Mater. Chem. A* **2014**, *2*, 13635–13640.
2. Sun, M.; Liu, H.J.; Liu, Y.; Qu, J.H.; Li, J.H. Graphene-based transition metal oxide nanocomposites for the oxygen reduction reaction. *Nanoscale* **2015**, *7*, 1250–1269. [[CrossRef](#)] [[PubMed](#)]
3. Sun, M.; Liu, H.J.; Qu, J.H.; Li, J.H. Earth-rich transition metal phosphide for energy conversion and storage. *Adv. Energy Mater.* **2016**, *6*, 1600087. [[CrossRef](#)]
4. Tiwari, J.N.; Vij, V.; Kemp, K.C.; Kim, K.S. Engineered carbon-nanomaterial-based electrochemical sensors for biomolecules. *ACS Nano* **2016**, *10*, 46–80. [[CrossRef](#)] [[PubMed](#)]
5. Wei, G.; Zhang, J.T.; Xie, L.; Jandt, K.D. Biomimetic growth of hydroxyapatite on super water-soluble carbon nanotube-protein hybrid nanofibers. *Carbon* **2011**, *49*, 2216–2226. [[CrossRef](#)]
6. Zhu, Y.W.; Murali, S.; Cai, W.W.; Li, X.S.; Suk, J.W.; Potts, J.R.; Ruoff, R.S. Graphene and graphene oxide: Synthesis, properties, and applications. *Adv. Mater.* **2010**, *22*, 3906–3924. [[CrossRef](#)] [[PubMed](#)]
7. Zhao, X.N.; Zhang, P.P.; Chen, Y.T.; Su, Z.Q.; Wei, G. Recent advances in the fabrication and structure-specific applications of graphene-based inorganic hybrid membranes. *Nanoscale* **2015**, *7*, 5080–5093. [[CrossRef](#)] [[PubMed](#)]
8. Chen, D.; Tang, L.H.; Li, J.H. Graphene-based materials in electrochemistry. *Chem. Soc. Rev.* **2010**, *39*, 3157–3180. [[CrossRef](#)] [[PubMed](#)]
9. Ding, J.W.; Zhu, S.Y.; Zhu, T.; Sun, W.; Li, Q.; Wei, G.; Su, Z.Q. Hydrothermal synthesis of zinc oxide-reduced graphene oxide nanocomposites for an electrochemical hydrazine sensor. *RSC Adv.* **2015**, *5*, 22935–22942. [[CrossRef](#)]
10. Wang, M.Y.; Shen, T.; Wang, M.; Zhang, D.E.; Chen, J. One-pot green synthesis of Ag nanoparticles-decorated reduced graphene oxide for efficient nonenzymatic H₂O₂ biosensor. *Mater. Lett.* **2013**, *107*, 311–314. [[CrossRef](#)]
11. Li, Y.; Zhang, P.P.; Ouyang, Z.F.; Zhang, M.F.; Lin, Z.J.; Li, J.F.; Su, Z.Q.; Wei, G. Nanoscale graphene doped with highly dispersed silver nanoparticles: Quick synthesis, facile fabrication of 3D membrane-modified electrode, and super performance for electrochemical sensing. *Adv. Funct. Mater.* **2016**, *26*, 2122–2134. [[CrossRef](#)]
12. Zhang, P.P.; Zhao, X.N.; Ji, Y.C.; Ouyang, Z.F.; Wen, X.; Li, J.F.; Su, Z.Q.; Wei, G. Electrospinning graphene quantum dots into a nanofibrous membrane for dual-purpose fluorescent and electrochemical biosensors. *J. Mater. Chem. B* **2015**, *3*, 2487–2496. [[CrossRef](#)]
13. Dong, H.F.; Gao, W.C.; Yan, F.; Ji, H.X.; Ju, H.X. Fluorescence resonance energy transfer between quantum dots and graphene oxide for sensing biomolecules. *Anal. Chem.* **2010**, *82*, 5511–5517. [[CrossRef](#)] [[PubMed](#)]
14. Wang, Y.; Li, Z.H.; Wang, J.; Li, J.H.; Lin, Y.H. Graphene and graphene oxide: Biofunctionalization and applications in biotechnology. *Trends Biotechnol.* **2011**, *29*, 205–212. [[CrossRef](#)] [[PubMed](#)]

15. Hu, K.S.; Kulkarni, D.D.; Choi, I.; Tsukruk, V.V. Graphene-polymer nanocomposites for structural and functional applications. *Prog. Polym. Sci.* **2014**, *39*, 1934–1972. [[CrossRef](#)]
16. Zhang, M.F.; Li, Y.; Su, Z.Q.; Wei, G. Recent advances in the synthesis and applications of graphene-polymer nanocomposites. *Polym. Chem.* **2015**, *6*, 6107–6124. [[CrossRef](#)]
17. Kuila, T.; Bose, S.; Mishra, A.K.; Khanra, P.; Kim, N.H.; Lee, J.H. Chemical functionalization of graphene and its applications. *Prog. Mater. Sci.* **2012**, *57*, 1061–1105. [[CrossRef](#)]
18. Georgakilas, V.; Otyepka, M.; Bourlinos, A.B.; Chandra, V.; Kim, N.; Kemp, K.C.; Hobza, P.; Zboril, R.; Kim, K.S. Functionalization of graphene: Covalent and non-covalent approaches, derivatives and applications. *Chem. Rev.* **2012**, *112*, 6156–6214. [[CrossRef](#)] [[PubMed](#)]
19. Georgakilas, V.; Tiwari, J.N.; Kemp, K.C.; Perrnan, J.A.; Bourlinos, A.B.; Kim, K.S.; Zboril, R. Noncovalent functionalization of graphene and graphene oxide for energy materials, biosensing, catalytic, and biomedical applications. *Chem. Rev.* **2016**, *116*, 5464–5519. [[CrossRef](#)] [[PubMed](#)]
20. Chen, D.; Feng, H.B.; Li, J.H. Graphene oxide: Preparation, functionalization, and electrochemical applications. *Chem. Rev.* **2012**, *112*, 6027–6053. [[CrossRef](#)] [[PubMed](#)]
21. Subrahmanyam, K.S.; Ghosh, A.; Gomathi, A.; Govindaraj, A.; Rao, C.N.R. Covalent and noncovalent functionalization and solubilization of graphene. *Nanosci. Nanotechnol. Lett.* **2009**, *1*, 28–31. [[CrossRef](#)]
22. Wang, J.H.; Ouyang, Z.F.; Ren, Z.W.; Li, J.F.; Zhang, P.P.; Wei, G.; Su, Z.Q. Self-assembled peptide nanofibers on graphene oxide as a novel nanohybrid for biomimetic mineralization of hydroxyapatite. *Carbon* **2015**, *89*, 20–30. [[CrossRef](#)]
23. Wang, J.H.; Zhao, X.J.; Li, J.F.; Kuang, X.; Fan, Y.Q.; Wei, G.; Su, Z.Q. Electrostatic assembly of peptide nanofiber-biomimetic silver nanowires onto graphene for electrochemical sensors. *ACS Macro Lett.* **2014**, *3*, 529–533. [[CrossRef](#)]
24. Yang, H.; Fung, S.Y.; Sun, W.; Mikkelsen, S.; Pritzker, M.; Chen, P. Ionic-complementary peptide-modified highly ordered pyrolytic graphite electrode for biosensor application. *Biotechnol. Prog.* **2008**, *24*, 964–971. [[CrossRef](#)] [[PubMed](#)]
25. Kim, S.N.; Kuang, Z.F.; Slocik, J.M.; Jones, S.E.; Cui, Y.; Farmer, B.L.; McAlpine, M.C.; Naik, R.R. Preferential binding of peptides to graphene edges and planes. *J. Am. Chem. Soc.* **2011**, *133*, 14480–14483. [[CrossRef](#)] [[PubMed](#)]
26. Katoch, J.; Kim, S.N.; Kuang, Z.F.; Farmer, B.L.; Nalk, R.R.; Tatulian, S.A.; Ishigami, M. Structure of a peptide adsorbed on graphene and graphite. *Nano Lett.* **2012**, *12*, 2342–2346. [[CrossRef](#)] [[PubMed](#)]
27. Cui, Y.; Kim, S.N.; Jones, S.E.; Wissler, L.L.; Naik, R.R.; McAlpine, M.C. Chemical functionalization of graphene enabled by phage displayed peptides. *Nano Lett.* **2010**, *10*, 4559–4565. [[CrossRef](#)] [[PubMed](#)]
28. Li, P.P.; Chen, X.; Yang, W.S. Graphene-induced self-assembly of peptides into macroscopic-scale organized nanowire arrays for electrochemical nadh sensing. *Langmuir* **2013**, *29*, 8629–8635. [[CrossRef](#)] [[PubMed](#)]
29. Fan, Z.J.; Wang, J.Q.; Wang, Z.F.; Li, Z.P.; Qiu, Y.N.; Wang, H.G.; Xu, Y.; Niu, L.Y.; Gong, P.W.; Yang, S.R. Casein phosphopeptide-biofunctionalized graphene biocomposite for hydroxyapatite biomimetic mineralization. *J. Phys. Chem. C* **2013**, *117*, 10375–10382. [[CrossRef](#)]
30. Wei, G.; Zhang, Y.; Steckbeck, S.; Su, Z.Q.; Li, Z. Biomimetic graphene-pept nanohybrids with high solubility, ferromagnetism, fluorescence, and enhanced electrocatalytic activity. *J. Mater. Chem.* **2012**, *22*, 17190–17195. [[CrossRef](#)]
31. Li, S.K.; Shen, Y.H.; Xie, A.J.; Yu, X.R.; Qiu, L.G.; Zhang, L.; Zhang, Q.F. Green synthesis of silver nanoparticles using capsicum annum l. Extract. *Green Chem.* **2007**, *9*, 852–858. [[CrossRef](#)]
32. Liu, S.; Tian, J.Q.; Wang, L.; Li, H.L.; Zhang, Y.W.; Sun, X.P. Stable aqueous dispersion of graphene nanosheets: Noncovalent functionalization by a polymeric reducing agent and their subsequent decoration with ag nanoparticles for enzymeless hydrogen peroxide detection. *Macromolecules* **2010**, *43*, 10078–10083. [[CrossRef](#)]
33. Fang, Y.X.; Guo, S.J.; Zhu, C.Z.; Zhai, Y.M.; Wang, E.K. Self-assembly of cationic polyelectrolyte-functionalized graphene nanosheets and gold nanoparticles: A two-dimensional heterostructure for hydrogen peroxide sensing. *Langmuir* **2010**, *26*, 11277–11282. [[CrossRef](#)]
34. Liu, S.; Tian, J.Q.; Wang, L.; Sun, X.P. A method for the production of reduced graphene oxide using benzylamine as a reducing and stabilizing agent and its subsequent decoration with ag nanoparticles for enzymeless hydrogen peroxide detection. *Carbon* **2011**, *49*, 3158–3164. [[CrossRef](#)]

35. Zhou, K.F.; Zhu, Y.H.; Yang, X.L.; Luo, J.; Li, C.Z.; Luan, S.R. A novel hydrogen peroxide biosensor based on au-graphene-hrp-chitosan biocomposites. *Electrochim. Acta* **2010**, *55*, 3055–3060. [[CrossRef](#)]
36. Xie, L.L.; Xu, Y.D.; Cao, X.Y. Hydrogen peroxide biosensor based on hemoglobin immobilized at graphene, flower-like zinc oxide, and gold nanoparticles nanocomposite modified glassy carbon electrode. *Colloids Surf. B* **2013**, *107*, 245–250. [[CrossRef](#)] [[PubMed](#)]



© 2017 by the authors; licensee MDPI, Basel, Switzerland. This article is an open access article distributed under the terms and conditions of the Creative Commons Attribution (CC BY) license (<http://creativecommons.org/licenses/by/4.0/>).